

# Modular High-Power Shunt-Interleaved Drive System: A Realization up to 35 MW for Oil & Gas Applications

Stefan Schröder<sup>‡</sup>, Pierluigi Tenca<sup>■</sup>, Tobias Geyer<sup>\*</sup>, Paolo Soldi<sup>‡</sup>, Luis J. Garcés<sup>‡</sup>, Richard Zhang<sup>♦</sup>,  
Tommaso Toma<sup>♦</sup>, Paolo Bordignon<sup>†</sup>

<sup>‡</sup> GE Global Research, <sup>♦</sup> GE Oil & Gas, <sup>■</sup> formerly with Ansaldo Sistemi Industriali, <sup>†</sup> Ansaldo Sistemi Industriali  
<sup>\*</sup> University of Auckland, New Zealand,

Stefan.Schroeder@research.ge.com, Pierluigi.Tenca@ieee.org, t.geyer@ieee.org, Paolo.Soldi@research.ge.com,  
Garcés@ge.com, zhangr@ge.com, Tommaso.Toma@ge.com, Paolo.Bordignon@asiansaldo.com

**Abstract**—The paper describes experimental results of a medium-voltage, modular, 35 MW drive for oil & gas applications realized by interconnecting voltage-source three-level converters equally sharing the motor current. Drives rated for tens of Megawatts are increasingly needed as torque helpers for gas turbines in the oil & gas industry and one envisions that they will replace them completely in the future. These drives must be very reliable, often capable of reversible power flow and high power quality when connected to weak grids in remote areas. The pronounced torsional eigenmodes of large compressors and gas turbines demand for very low torque harmonic content.

**Keywords**—multilevel converter; neutral-point clamped converter; modular converter; interleaving; synchronous machine drive; medium-voltage drive; active rectifier

## I. INTRODUCTION

Electrical drives rated for tens of Megawatts and rotational speeds around 3000 rpm are increasingly needed in the oil & gas industry, especially in high-power compressor trains for Liquefied Natural Gas (LNG). The present role of these drives is to act as starter and helper for the prime movers of the compressor trains. Nowadays, such prime movers are still constituted by gas turbines, but it is envisioned that they will be entirely replaced by variable frequency drives [1]. Due to the required power levels, the machine is often synchronous with a classical field winding, smoothed poles and a mandatory brushless exciter to meet the safety requirements for explosive environments. Because of the considerable economic value of LNG processes, such drives must be characterized by a very high reliability and availability for continuous duty. Moreover, they must feature a low harmonic content in the currents drawn from the grid and in the motor torque. The latter is of fundamental importance because of the lowly damped torsional eigenmodes of the mechanical shaft comprising a large gas turbine, compressors and the synchronous machine. Often, also a reversible power flow between the electrical machine and the grid is required.

This paper describes a medium-voltage modular synchronous machine drive conceived for oil & gas applications. As shown in Figure 2, the drive is realized by paralleling up to four three-level Neutral-Point Clamped (NPC) converters. This leads to up to 35 MW shaft power. By interleaving, i.e. by properly phase-shifting the PWM equivalent carriers of the four converters, waveforms of very high quality are achieved both on the grid and on the machine side. Selected experimental results acquired during the full-scale product validation campaign are presented to highlight the benefits.

## II. CHOICE OF DRIVE SYSTEM CONCEPT

As outlined above, the main requirements in the targeted oil & gas applications are very high power (tens of Megawatts), very low torque and grid harmonics and high availability.

### A. High-Power Drive Options

Thyristors are available at very high power ratings. Furthermore, series connection is relatively simple and a proven approach. By using additional thyristor devices, redundancy can be easily implemented. Therefore, they are commonly used in Line-Commutated Inverters (LCI) for very high power applications. However, they can switch only once per fundamental cycle. Hence, the achievable power quality is comparatively poor. This typically implies the installation of bulky and expensive grid-side filters, which require careful design and tuning. Filters on the variable frequency machine side are typically not practical. Hence, thyristors are not attractive for a high torque quality drive application as considered here.

Consequently, only self-commutated topologies, which need fully controllable semiconductor devices, are considered in the following. The available voltage and current ratings of these devices have increased significantly in the recent past. Nevertheless, the targeted power level cannot be achieved with state of the art semiconductors in a standard topology, e.g. 2 or 3-level converters using one semiconductor per switch

position. For example, the power of a typical high-power, medium-voltage drive based on a 3-level NPC converter using 4.5 kV and 4 kA Integrated Gate Commutated Thyristors (IGCTs) is rated at approximately 10 MW.

Hence, it is mandatory to use several semiconductor devices in series or parallel connection. This could be done at the device level by using direct series or parallel connections, where these devices are switched synchronously.

Alternatively, multi-level topologies can be chosen to increase the achievable voltage level compared to 2-level inverters. Also here, several devices are effectively connected in series and the additional degrees of freedom allow for switching these devices independently. This increases both the available number of discrete voltage levels and the effective switching frequency. As a result, the voltage harmonics can be reduced thus directly improving the current and torque quality.

As a third option, complete converter modules can be paralleled (or series connected using isolation transformers). This option can also be used to enhance the achievable output performance, as it will be highlighted in the consecutive sections.

The use of more semiconductors can address the power requirement and improve the power quality by using suitable topologies. However, as a drawback, the part count of the system is increased with consequent greater likelihood of failures and reduced system reliability. As a countermeasure, some kind of redundancy is generally required in these systems in order to fulfill the stringent system availability requirements common in the oil & gas industry.

In summary, it can be seen that standard converter solutions do not satisfactorily address all three requirements, i.e. power level, power quality and availability.

### B. Selection of Switching Component

At high power levels, typically either Insulated Gate Bipolar Transistors (IGBTs) or IGCTs are used nowadays in self-commutated converters. IGBTs are dominating in drives with lower to medium power levels, since at lower voltages they facilitate very fast switching frequencies. However, higher blocking voltage IGBTs have increased conduction and switching losses. Hence, the achievable switching frequency and the maximum current capability of a single device usually decrease. As a result, the maximum power that can be handled by a single device is almost constant or even decreases with increasing blocking voltages. This scenario renders IGCTs more attractive for higher voltage and power levels at the present time, since they offer higher power capability per device, which reduces the component count and finally leads to a higher reliability for the overall system. Consequently, in the drive system described here a 4.5 kV 4 kA IGCT was chosen as switching device. As it will be detailed later, such a high power rating allows one to achieve the drive requirements, namely power level and power quality, at a comparably low part count as a basis for high reliability.

### C. Selection of Drive Topology

As already mentioned, multi-level topologies can increase both the power level and the output performance of a converter. Well known options are the Diode Clamped (DC), Flying Capacitor (FC) and the Cascaded Cell (CC) topologies, which use different concepts to balance the voltages among the switches.

The high power level considered here would require a high level number, which would pose significant hurdles on each of the topologies above – namely, the balancing of the tapped dc-link voltages, the size of the ‘flying caps’ or the multiple isolated power supplies for DC, FC or CC topologies, respectively. Hence, a shunt interleaved converter topology is chosen, where up to four independent 3-level NPC converters are connected via individual inductors to the three-phase machine. This allows the converters to switch independently from each other, thereby enabling a higher output performance when compared to the single or hard paralleled converters. The chosen modular topology is based on standard high-power converter units that are able to work independently from each other. This feature leads to an elegant way to realize a redundant drive system. The detailed working principle of the system is explained in the following section.

### III. TOPOLOGY AND MAIN FEATURES OF THE MODULAR DRIVE SYSTEM

The modular structure of the chosen drive system topology is shown in Figure 2 [1] - [7]. The four converters are connected to the grid and to the machine using individual

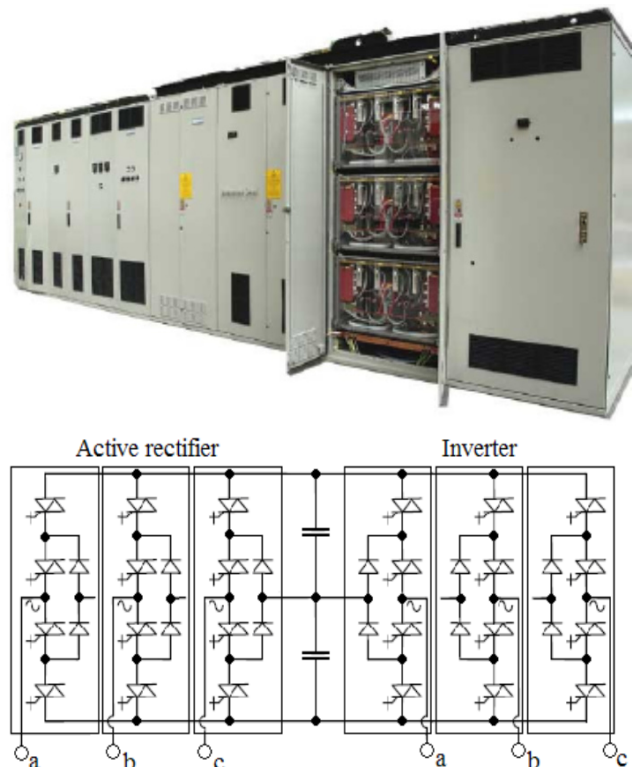


Figure 1: Silcovert GN converter (Ansaldo Systemi Industriali) (above) Three-level NPC AC/DC/AC topology constituting each of the four converter modules (below)

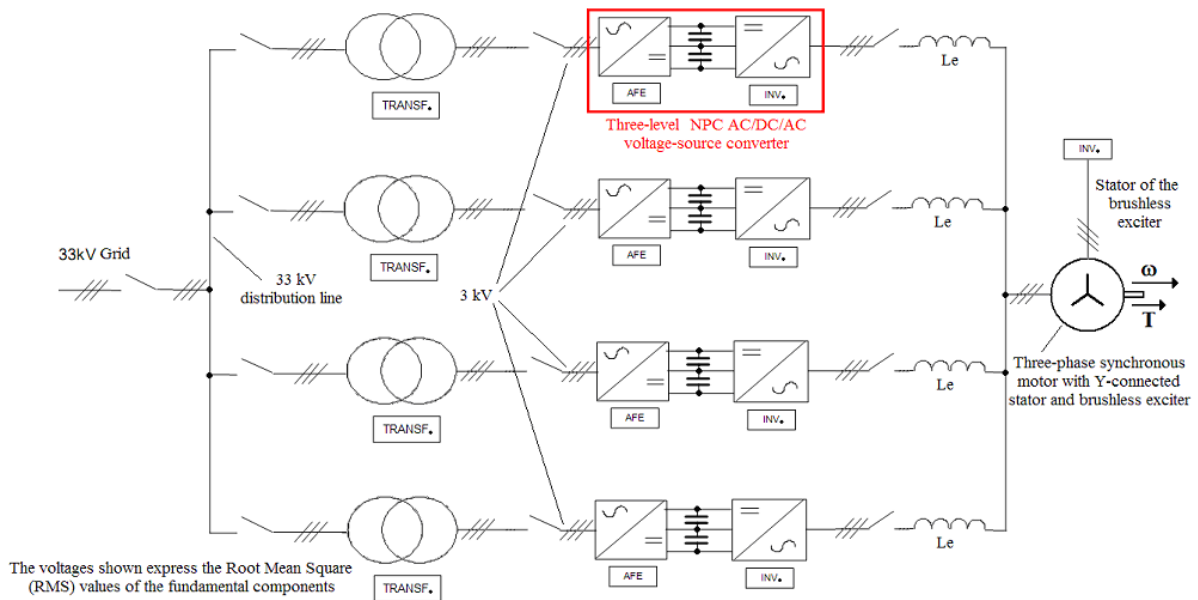


Figure 2: System diagram highlighting the structure, the interconnection with the grid and the machine and the most relevant electrical quantities

transformers and inductors, respectively. In this paper, each of the separate channels is called a “thread”, which comprises a transformer, a converter and the machine side inductor.

At the machine side, the equal sharing of the fundamental machine phase currents among the inverters, and machine phase currents with very low harmonic content are achieved through two main techniques: First, by proper synchronization and phase interleaving (as described in the next section) among the equivalent PWM carriers of the individual inverters, as well as by proper inverter control. Second, by proper design of the machine side coupling inductances  $L_e$ . On the grid side, the same approach is used exploiting the purposely designed built-in stray inductances of the transformers.

The four-pole synchronous machine, rated for a fundamental frequency of 100 Hz, possesses a standard three-phase Y-connected stator. Its rotor field winding is fed by an integrated brushless exciter using a rotating three-phase diode

bridge. The stator of the brushless exciter is fed by a low-voltage two-level voltage-source inverter. The machine and the converters satisfy the standards for operation in explosive environments. The four-pole machine used in the installation was operated up to 110 Hz fundamental frequency, i.e. 3300 rpm. Using a two-pole machine, this corresponds to 6600 rpm.

The air core (iron-less) coupling inductors, the machine and the 33 kV / 3 kV transformers have inverter-grade insulation. Figure 1 shows the well-known NPC topology constituting each converter and a picture of the Silcovert GN converter used within this project. During the test campaign, the drive system was connected to the grid by a 132 kV / 33 kV interconnection transformer.

The modulated phase voltages, arising from the use of synchronous PWM, are shown in Figure 3 for one active rectifier at 50 Hz fundamental frequency and for one inverter (INV) at 100 Hz, respectively. The voltages are measured with respect to the DC-link mid point. Due to the phase shifting of the carriers, which is a characteristic feature of interleaving, the switching patterns among the threads differ. Consequently, the thread patterns are typically different from the ones in single converter drives, e.g. lacking the typically chosen pulse symmetry. Yet, as it can be seen subsequently, the resulting harmonic performance in the grid and machine currents is superior.

Each converter has its own independent controller and is capable of autonomous operation if necessary. This was a pivotal design requirement to enhance the system availability in case of failures. In addition, the converters must communicate and operate as a whole. These features have required the development of a control architecture based on a sophisticated distributed hardware and software scheme. Any number of failed threads can be isolated from the rest of the system by the breakers located on the grid and the machine side. The remaining threads can still operate in this degraded

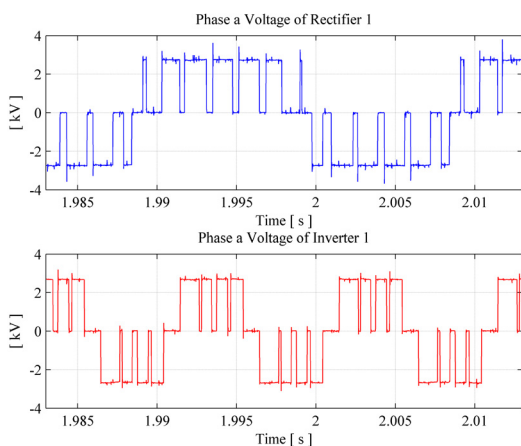


Figure 3: Measurements of phase A voltages of the Active Rectifier 1 (above) and Inverter 1 (below) when synchronous PWM modulation is used for both (cf. Figure 8 and Figure 9)

mode where the phase shifting of the interleaved carriers is adjusted to the number of remaining threads and the total available power is reduced accordingly. However, the detailed discussion of this degraded mode operation and the impact on system availability are beyond the scope of this paper.

#### IV. INTERLEAVING CONCEPT

The basic concept of interleaving relies on the common connection point (e.g. the motor voltage) ‘seeing’ the average of the individual converter voltages. By suitable modification of each converter voltage pattern, the (desired) fundamental voltages are constructively added and certain (undesired) harmonics are destructively added, i.e. cancelled.

##### A. Single-Phase Equivalent Circuit

To illustrate the concept of ‘averaging’ the voltages, a simplified single-phase (differential mode) equivalent circuit of  $k$  parallel inverters connected to the machine is shown in Figure 4 a). The inverter single-phase voltages  $V_{INV\ i1}$  shown in this picture represent only the differential mode part of the inverter voltages. Hence, common-mode effects are not visible in this simplified equivalent circuit anymore. However, in the considered drive system, common-mode currents are inhibited anyway as will be detailed in subsection C.

The inverters can be represented by an ideal voltage source with their average voltage  $V_{INV\ AVG1}$  in series with the parallel connection of all the inverter impedances. This Thevenin equivalent circuit is shown in Figure 4 b). With the quantities defined as shown in this figure, the resulting machine phase voltage  $V_{M1}$  can be calculated according to:

$$V_{M1} = \frac{Z_M}{Z_M + Z_{INV} / k} V_{INV\ AVG1} + \frac{Z_{INV} / k}{Z_M + Z_{INV} / k} V_{EMF1} \quad (1)$$

with  $V_{INV\ AVG1} := \frac{1}{k} \sum_{i=1}^k V_{INV\ i1}$

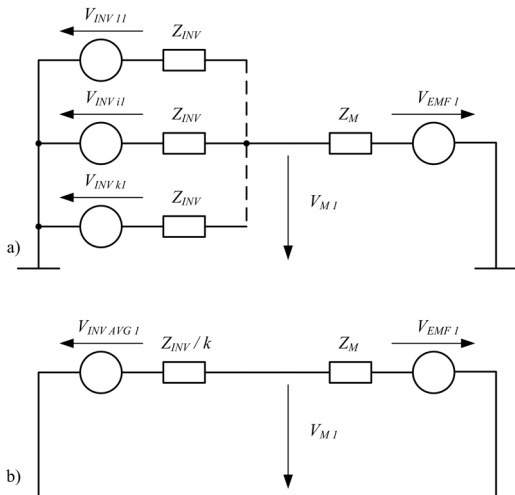


Figure 4: a) Single-phase equivalent circuit of  $k$  parallel inverters connected to a machine b) Thevenin equivalent of the parallel inverters

Hence, the total effect of the inverters on the machine voltage (and current) can be described by the average of the  $k$  inverter phase voltages  $V_{INV\ AVG1}$ .

In the next subsection, we will describe an approach to cancel undesired voltage harmonics in the voltage  $V_{INV\ AVG1}$  representing the effect of the inverters on the machine. Subsequently, key aspects of the inductor sizing are discussed. Finally, additional filter effects of the inductors are highlighted.

##### B. Harmonic Cancellation

The harmonic spectrum of PWM converters is characterized by integer multiples of the fundamental frequency  $f_0$  and the carrier frequency  $f_c$ . According to [8], each harmonic  $h_{mn}(t)$  can be written as:

$$h_{mn}(t) = C_{mn} \cos(m(2\pi f_c t + \theta_c) + n(2\pi f_0 t + \theta_0) + \theta_{mn}) \quad (2)$$

Here,  $\theta_c$  and  $\theta_0$  are the phase of the carrier and the fundamental, respectively;  $C_{mn}$  and  $\theta_{mn}$  are expressions depending on the modulation scheme;  $m$  and  $n$  are integer constants. Please note that different combinations of  $m$  and  $n$  can result in the same harmonic frequency, especially when synchronous PWM is used. In the PWM voltage spectrum, the (geometric) sum of all harmonic components described by (2) is visible. According to [9], even values of  $m$  are paired with odd values of  $n$  and vice versa for 3-level phase disposition natural sampled PWM. All other combinations yield zero amplitudes of the corresponding harmonic. Practical modulator implementations based on space-vector PWM show to behave qualitatively similar to this.

An important conclusion from (2) is that the amplitude  $C_{mn}$  of a certain harmonic does not change if the phase of the fundamental and/or the carrier is changed. Under this condition, only the phase  $\theta_{h_{mn}}$  of the harmonic is changed according to:

$$\theta_{h_{mn}} = m\theta_c + n\theta_0 + \theta_{mn} \quad (3)$$

The value of  $n$  also decides about the nature of the resulting harmonic. If  $n$  is an integer multiple of 3 (including zero), this harmonic generates a common mode voltage. Whereas, for all other cases it generates a differential mode voltage [8]. The reason for this stems from the definition of the common mode voltage as the arithmetic average of the three phase voltages, i.e. their sum divided by three. Each individual phase voltage has a fundamental phase shift  $\theta_0$  of  $0^\circ$ ,  $120^\circ$  and  $240^\circ$ , respectively. Hence, the sum of the three harmonics corresponding to each individual phase, is non-zero exactly only under the condition that  $n$  is a multiple of 3.

In the interleaved system, each PWM unit uses the same fundamental and carrier frequencies but the phase of the carrier differs for each converter. By choosing the phases  $\theta_{c_i}$  for each converter  $i$ , certain classes of harmonics can be cancelled. The harmonics of each thread are the same but phase shifted by  $m\theta_{c_i}$  according to (3). Considering the four thread system described in this paper and using the phases

$$\theta_{C1} = 0^\circ, \theta_{C2} = 45^\circ, \theta_{C3} = 90^\circ, \theta_{C4} = 135^\circ, \quad (4)$$

all harmonics with  $m=2, 4, 6$  (for all  $n$ , i.e. including their sidebands) are cancelled and harmonics with  $m=1, 3, 5, \dots$  are reduced but not cancelled. The cancellation of the harmonics in the output voltage (and hence the output current) is independent of the value of the connecting inductors and relies solely on the averaging of the individual converter voltages as already shown in subsection A.

### C. Inductor Sizing

The main purpose of the inductors is to limit the cross-currents between the threads, which is discussed in the following paragraphs. The  $i$ -th cross-current is defined as the  $i$ -th thread current minus the arithmetic average of all thread currents. To achieve a cancellation (or reduction) in the output voltage, the corresponding harmonics of each thread must necessarily be phase shifted against each other as outlined above. Consequently, the resulting voltage difference among the threads will drive cross-currents between them. The amplitude of these currents is limited by introducing properly sized inductors. The design of the inductors is dominated by the currents in the order of the switching frequencies. For frequencies far beyond the switching frequencies the impedance of the inductor is significantly increased and the cross-currents are negligible. For currents well below the switching frequency (including also the fundamental frequency and dc) the impedance of the inductors is small and less effective. However, the individual current controllers of the threads can ensure an equal current sharing here.

It is important to note that in the system considered here only differential mode cross-currents can flow between the threads. Common mode currents (on both sides) are inhibited by the galvanic isolation provided by the transformers on the input side. This yields the following advantages: firstly, only differential mode harmonic voltages need to be considered in the inductor design. Hence, the large common mode harmonic at  $f_C$  cannot drive any currents. Secondly, the cross-currents on the grid and on the machine side are completely independent of each other, which simplifies both the analysis and the control. Thirdly, since the thread currents are pure differential mode currents, a three-phase differential mode inductor could be used. However, the latter option is not employed here but single-phase, air-core inductors are used instead. The advantage is that they maintain their inductance also under severe failure conditions that may impose common mode currents in the threads.

The cross-currents increase the RMS value of the thread

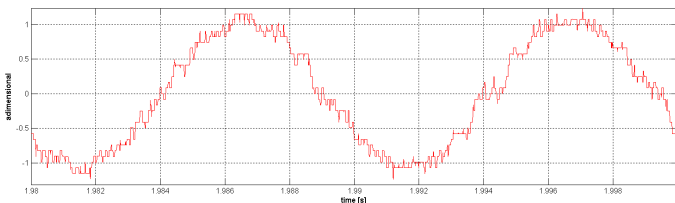


Figure 5: Example of average inverter voltage  $V_{INV\_AVG1}$  (post-processed measurements, normalized)

currents and hence the losses. However, the cross-currents are composed of different harmonic frequencies as explained in subsection B. Hence, they are orthogonal to the main fundamental currents and the change in the RMS value is rather small even for high cross-current values. Consequently, instead of focusing on the RMS value, only the current ripple is typically considered in order to keep the peak current of each thread below a certain threshold.

The dominant cross-current harmonic frequency is the first side band at twice  $f_C$ . The same side-band harmonic is also the dominant harmonic seen in the current of traditional single-thread (or non-interleaved) inverters. On the grid side, this current is limited by proper choice of the transformer stray inductance in standard (i.e. non-interleaved) converters. Here, the stray inductance of such converter-transformers is also sufficient to limit the cross-currents on the grid side in this system. On the machine side, the required inductor values are similar.

The voltage drop across the inductor reduces the available output voltage. However, this effect shows to be less critical than it may be perceived. The main reason is that the synchronous motor is operated at (or close to) unity power factor (PF) to optimally utilize the machine. This choice implies that the voltage drop across the inductor and the machine voltage are orthogonal to each other. As a consequence, the effect on the voltage amplitude of the inverter is rather small even for relatively large inductor impedances. Even for a 25% pu (per unit) impedance, the increase in the converter voltage  $V_{Conv\ pu}$  is only 3% at the nominal drive operating point:

$$V_{Conv\ pu} = \sqrt{100\%^2 + 25\%^2} = 103\%. \quad (5)$$

### D. Additional Filter Effects

An example of waveform for the average inverter voltage  $V_{INV\_AVG1}$  with 4 interleaved threads is shown in Figure 5. This voltage already shows a very good approximation of a sine wave. It has significantly finer and more voltage steps than the voltages commonly known from a single NPC converter. In fact, this voltage exhibits strong similarities to a 9-level converter pattern. If such a pattern were directly applied to an electrical machine, its inductive impedance would act as a low-pass filter resulting in an even smoother machine current. Such a well-know low-pass behavior is further pronounced in this system. As discussed earlier, the parallel connection of the four inductors is effectively seen in series to the machine impedance as can be observed in Figure 4 b). This results in a higher attenuation. It should be noted that although the inductance of a synchronous machine is high at the fundamental frequency (in the order of 1 pu), it is typically significantly smaller at higher frequencies, e.g. due to the effect of the damper windings [11]. That means that the relative increase of the total inductance by the additional coupling inductors helps to further dampen the remaining harmonic frequencies in the average voltage  $V_{INV\_AVG1}$  of the inverters.

Another interesting and correlated effect is the additional smoothing of the machine voltage. When the machine impedance is significantly lower than the parallel impedance of the inductors, the corresponding harmonic content of the average inverter voltage on the machine terminal is attenuated according to (1). The result of this filter effect can be clearly observed in the very smooth measured machine voltage waveforms that are shown in the validation section.

## V. CONTROL

The structure of the control hardware is designed such that it allows for a high availability of the overall drive system. This is achieved by equipping each thread with its own dedicated control hardware, which is identical for all four threads. The control units can act independently from each other – e.g. a failure in one thread does not affect the operability of the other threads’ control units. The coordination and the data exchange among the four independent threads are enabled by a “reflective memory” scheme. Specifically, a given fraction of the control units’ local memory is allocated as “reflective memory”. When new data is written into this fraction of the control unit’s memory, the changes are propagated to the memory of the other units via fiber optics. Provided that data is changed consecutively, the reflective memory acts as a single virtual memory unit that is physically located inside and accessible by each of the four threads control units. This concept allows for seamless data exchange between the thread controllers while ensuring a high availability.

The control software is identical for all four threads. It consists of two main parts – a machine and a current controller for each thread. The machine controller is based on a state-of-the-art field oriented control scheme working in a stator-flux oriented orthogonal coordinate system. The torque reference is translated into a torque producing current reference, while flux errors are mapped into an orthogonal flux producing current reference. In steady state the machine is completely fluxed via the field current supplied by the brushless exciter.

The two orthogonal current references of the machine controller are divided by the number of threads and passed to the local thread current controllers. The latter regulate the thread currents independently from each other using measurements of the thread currents for feedback. The output of the thread current controller is a space vector. Each thread

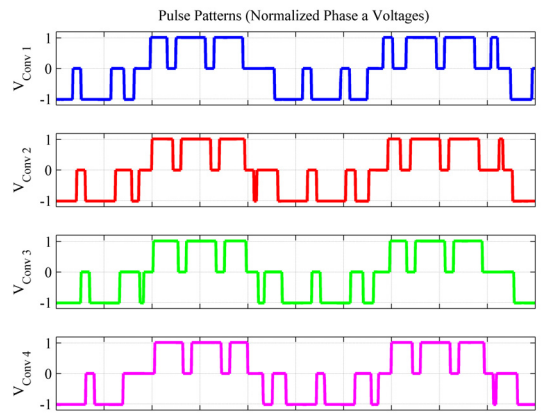


Figure 6: Converter voltage pulse pattern of the same phase at four threads illustrating the interleaving principle (simulation)

features a Pulse Width Modulator (PWM) that drives the IGBTs of the thread inverter by synthesizing an appropriate switching pattern. The switching pattern can be asynchronous, implying that the PWM runs with a fixed switching frequency, or synchronous, where the PWM frequency is a multiple of the fundamental frequency and where the equivalent PWM carrier is synchronized with the fundamental’s phase.

Since each thread controller acts locally, fluctuations in the dc-link voltage and/or variations in the inductors are accounted for locally. This ensures that within the controller bandwidth the four thread currents are of equal magnitude. Hence, uncontrolled low-frequency cross-currents between the threads are avoided.

To implement the interleaving scheme, the four thread controllers use the same sampling interval  $T_{S,Thread}$ , but they sample and act at time-instants shifted in time with respect to each other (e.g. a quarter of a sampling interval for 4 threads). The sampling occurs twice within each equivalent PWM carrier period. The developed interleaved thread real-time control executes the machine vector control algorithm locally on one thread control unit at a time. This means that the machine vector control execution is passed consecutively from one thread controller unit to the next thread controller unit. This gives rise to a virtual master controller that is physically handed over from one thread control unit to the next one. Hence the machine controller runs at four times the sampling frequency of the thread current controllers, i.e. at the interval  $T_{S,Machine}$ . The resulting timing of the control tasks is depicted in Figure 7. Figure 6 shows typical interleaved voltage pulse patterns that are generated in each of the 4 threads and refer to the same phase.

In addition to the harmonic benefits outlined above, interleaving can also improve the control performance with respect to non-interleaved control, where all four threads run at the same time-instants. The controller can react faster since the machine controller runs at four times the rate of the thread current controllers, and the thread controller execution is spread within the sampling interval. However, this additional feature is not further analyzed since it was not required for the targeted applications.

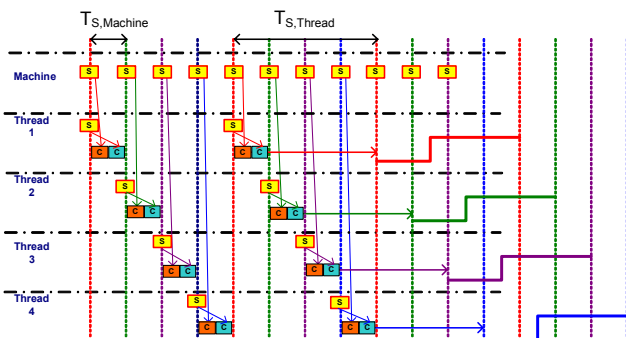


Figure 7: Control timing showing machine and thread control, where ‘s’ denotes the sampling instants and ‘c’ the computational steps

In the current system, each of the four threads is equipped with an active rectifier that allows drive operation also in full regenerating mode. Each active rectifier independently controls its dc-link voltages. The corresponding control cycle runs synchronously to the grid frequency, i.e. employs synchronous PWM. Proper phase shifting of the control tasks among the threads allows for interleaved operation similar to the machine side.

Summarizing: the control concept relies on four independent thread control units that exchange data by one single virtual memory (realized with a reflective memory scheme). In a field-oriented controller setting, the machine (virtual master) controller sets the thread current references, while the thread (slave) controllers regulate their thread currents. Interleaving greatly enhances the waveform of the machine current. The use of four independent threads with four independent control units ensures a high level of availability. Neither a physical master controller nor a central memory unit

is required due to the sequential execution of the machine vector control algorithm on the local thread controllers via the reflective memory scheme for data exchange.

## VI. SELECTED EXPERIMENTAL RESULTS

During the development and validation procedure, the drive system was tested in various ways: extensive computer simulations in Saber and Matlab, tests on a scaled-down drive system, full power tests of single phase legs and of the converters and finally full-scale system tests. Details of the complete validation approach are described in [1]. Here, selected characteristic results of the full-scale system tests are shown.

Figure 12 and Figure 13 show two views of the full-scale drive system at a test site of GE Oil & Gas in Massa, Italy. In Figure 12, the synchronous machine and the four converter units can be seen. Figure 13 shows a gas turbine, a synchronous generator and a resistor bank that were used to

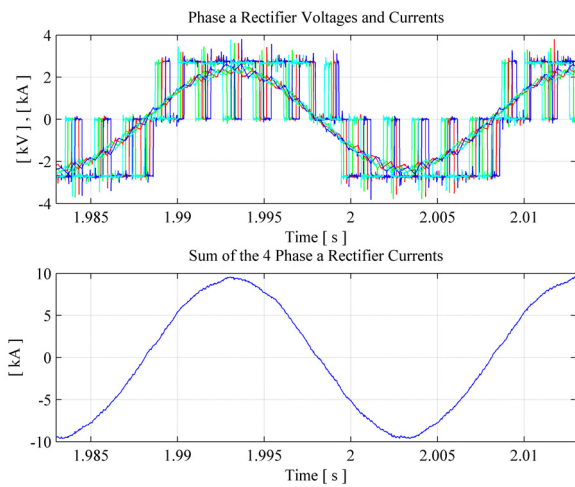


Figure 8: Measured phase A voltages and currents of the interleaved active rectifiers at 34 MW motoring operation mode (above); sum of their phase A currents (below)

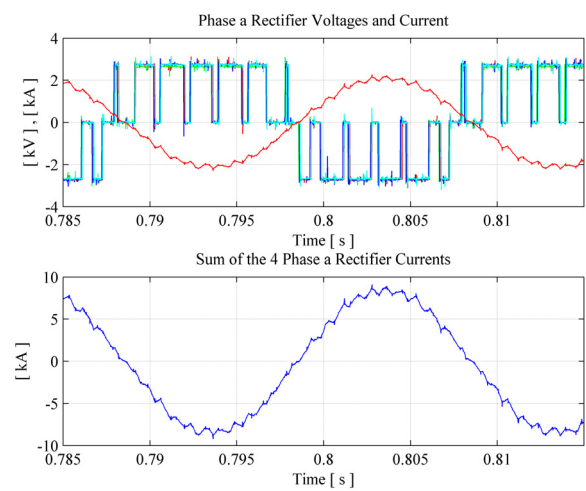


Figure 10: Measured phase A voltages and currents of the non-interleaved active rectifiers at 31 MW regenerating operation mode (above); sum of their phase A currents (below)

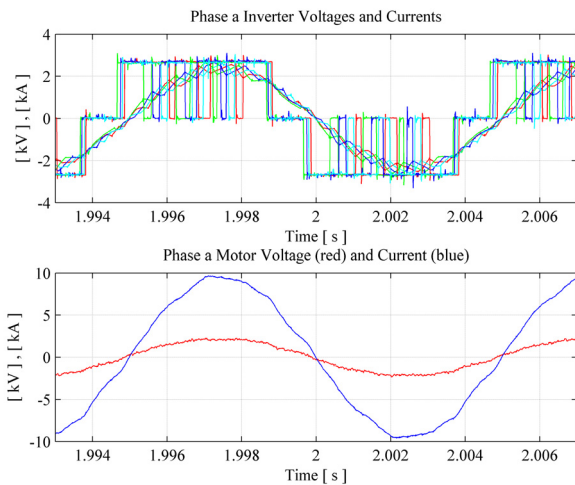


Figure 9: Measured phase A voltages and currents of the inverters (above) and the machine (below), respectively, at 34 MW motoring operation mode at 3000 rpm (100 Hz)

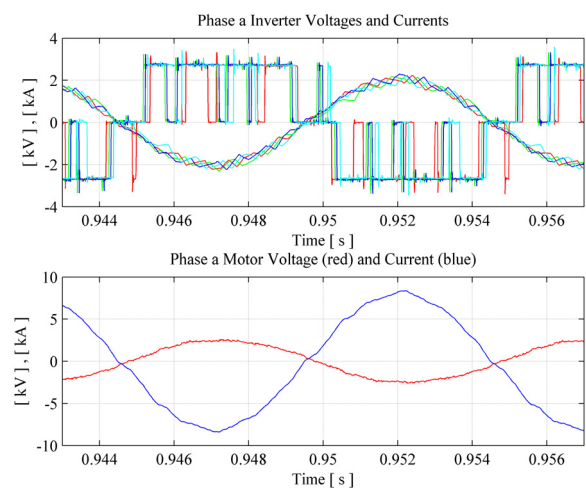


Figure 11: Measured phase A voltages and currents of the inverters (above) and the machine (below), respectively, at 31 MW regenerating operating mode at 3000 rpm (100 Hz)



Figure 12: View of the test setup showing the converters, inductors, the synchronous machine and the generator used to load the drive system during testing

test and validate the electrical drive system in generator and motor mode.

In order to validate motoring operation, the drive was connected to the load synchronous generator, which, in turn, was loaded with the resistor bank. Figure 8 and Figure 9 show typical waveforms captured during operation at 3000 rpm, i.e. 100 Hz fundamental electrical frequency, when the drive was drawing 34 MW from the grid and delivering 32 MW to the resistive load. Here (and also in Figure 10 and Figure 11), positive currents reflect currents flowing from the grid into the active rectifiers, and from the inverters to the machine, respectively.

Both the active rectifiers and the inverters were operating interleaved and ran synchronous PWM. Figure 8 refers to grid side. The upper plot depicts the phase A currents for each individual rectifier. Each of them exhibits the typical ripple, which, however, is phase-shifted with respect to each other. As a result, as depicted in the lower plot, the four ripples almost perfectly cancel out in the total grid current, which is equivalent to the sum of the four active rectifier currents.

Equivalently, Figure 9 shows the effect of interleaving on the machine side. Here again, the sum of the single inverter phase currents leads to a near sinusoidal machine phase current. Additionally, the very smooth machine voltage helps to further reduce the losses in the machine. In the operating point shown, the flux was smaller than nominal proving a significant current capability margin while validating also the overall cooling system.

In the framework of an additional test campaign, the drive was connected to a gas turbine replicating a typical LNG train setup, which also allowed the validation of the regenerative mode of operation. Figure 10 and Figure 11 depict selected waveforms of the active rectifiers and the inverters,

respectively, which were recorded at 3000 rpm with 31 MW fed into the grid. Unlike above, the interleaving of the active rectifiers was disabled. The absence of interleaving among the rectifiers renders their corresponding phase currents almost identical. Therefore, only one rectifier phase current is shown in the upper graph of Figure 10. The lower graph of Figure 10 shows the sum of the four rectifier phase A currents, which clearly exhibits the same ripple as the individual currents. A direct comparison with the grid current waveform shown in Figure 8 underlines the significant improvements achieved by interleaving.

The machine side quantities for regenerative operation are shown in Figure 11. Here the inverters are operating interleaved but with asynchronous PWM. As it can be seen, also in this case the motor phase current and voltage are almost sinusoidal.

## VII. CONCLUSIONS

The topology, the main features and the interleaving principle were described for a modular drive system composed of four IGCT-based 3-level NPC converters. Typical test results on the full-scale system in motoring and regenerative operation were shown. The interleaving control strategy delivers an excellent grid and output quality and an optimized performance that improves the characteristic and operability of large electrical drives required e.g. for oil & gas applications. Given the high power, this output performance is a remarkable achievement –particularly when compared to the present state of the art for drives based on voltage-source converters or LCIs. The drive system is based on standard industrial converter units using high power IGCT devices as a basis for high reliability. The fully modular system concept allows one to further improve the system availability by the use of redundancy. The same drive configuration can be extended to

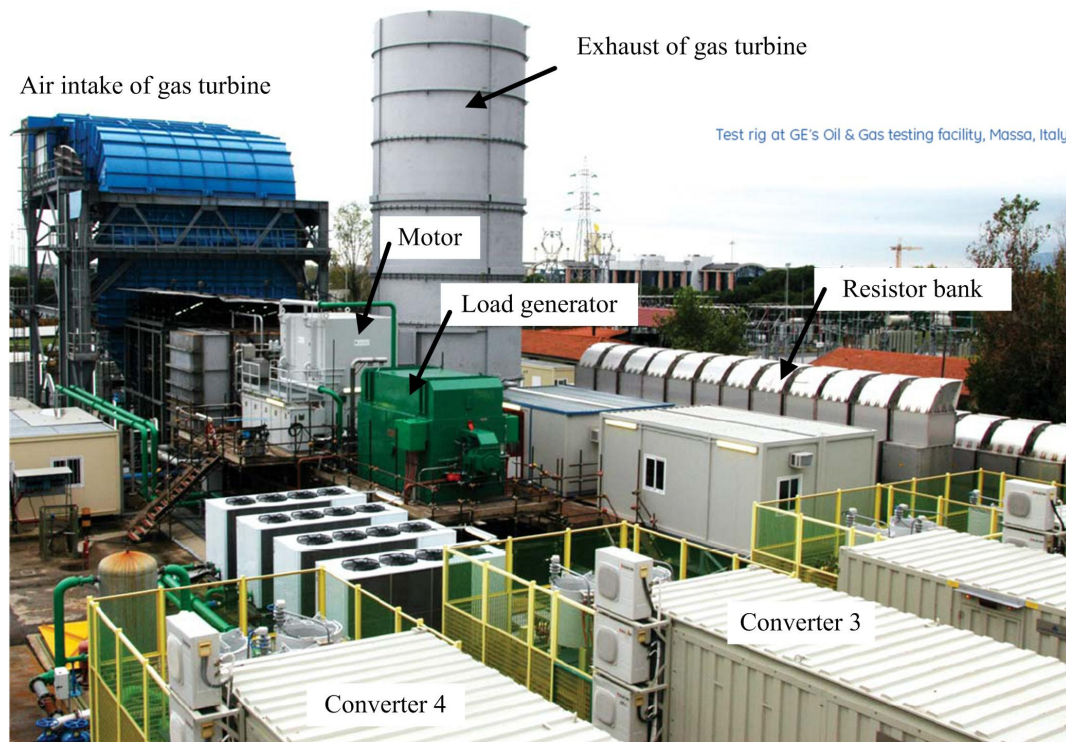


Figure 13: View of the test setup showing the drive system, load generator, its resistor bank and gas turbine

even higher power levels by increasing the single thread power density and the NPC converter output voltage. The described drive system is commercially available under the product family name Steadfast 40 [10].

#### VIII. ACKNOWLEDGMENTS

The authors would like to express their gratefulness to the people involved in this project for their valuable contributions and support during both the development and validation phase. Specifically, these people include Giuseppe Ferrari, Roberto Moleri, Mauro Perna, Alberto Tessarolo and Silvano Tola from Ansaldo Sistemi Industriali (ASI), as well as Massimiliano Alvino, Roberto Baccani, Roberto Biondi, Paul Decicco, Cyrus Harbourt, Allen Ritter, Rajarshi Sen, Christof Sihler, Joseph Song and Parag Vyas, who are with General Electric (GE). Additionally, the authors would like to acknowledge the support of the following persons: Alessandro Alaia, Fulvio Boattini, Matteo Carpaneto, Enzo Ciulin, Alberto Coffetti, Dario Colombo, Stefano D'Arrigo, Rajib Datta, Stefano Del Puglia, Amr Elaguizy, Carlo Gallant, Teresa Gargano, Andrea Iuretig, Paolo Masini, Ivo Pascolo, Michele Povolero, Alberto Roda, Robert Rösner, Marco Ruggiero, Paolo Segarich, Pietro Serra, Fahran Shakil, Mark Shepard and Francesco Soso.

#### REFERENCES

- [1] R. Baccani, R. Zhang, T. Toma, A. Iuretig, M. Perna: "Electric systems for high power compressor trains in oil and gas applications – system design, validation approach and performance", 36<sup>th</sup> Annual Turbomachinery Symposium. Houston, Texas, September 10-13, 2007
- [2] B. Shi, G. Venkataramanan: "Parallel operation of voltage source inverters with minimal intermodule reactors", Industry Applications Conference, 2004. IAS' 04. 39<sup>th</sup> IAS Annual Meeting, Volume 1, 3-7 Oct. 2004, pp: 162–165.

- [3] C. Liangliang, X. Lan, Y. Yangguang: "A novel parallel inverter system based on coupled inductors", 25<sup>th</sup> International Telecommunications Energy Conference, 2003. INTELEC' 03. 19-23 Oct. 2003, pp: 46 – 50.
- [4] L. Xiaosi, X. Rui: "Research on generating and restraining of circulating currents between parallel inverters", Power Elect. , No. 33, Vol. 3, 1999, pp. 16 - 18.
- [5] K. Matsui, F. Ueda, K. Tsuboi, K. Iwata, T. Kobayashi: "Parallel connections of pulsewidth modulated NPC converters using current sharing reactors", 22<sup>nd</sup> Industrial Electronics, Control, and Instrumentation Conference, 1996, IECON' 96 Vol. 3, pp. 1776 - 1783.
- [6] F. Ueda, K. Matsui, M. Asao, K. Tsuboi: "Parallel-connections of pulsewidth modulated inverters using current sharing reactors", IEEE Transactions on Power Electronics, Volume: 10, Issue: 6, Nov. 1995, pp: 673 - 679.
- [7] T. Kawabata, S. Higashino: "Parallel operation of voltage source inverters", IEEE Transactions on Industry Applications, Volume: 24, Issue: 2, March-April 1988, pp: 281 - 287.
- [8] D. G. Holmes, B. P. McGrath, "Opportunities for Harmonic Cancellation with Carrier-Based PWM for Two-Level and Multilevel Cascaded Inverters" in IEEE Transactions on Industry Applications, Vol. 37, No. 2, March-April 2001
- [9] D. G. Holmes, T. A. Lipo, "Pulse Width Modulation For Power Converters – Principles and Practice", IEEE Press, 2003, ISBN 0-471-20814-0
- [10] [http://www.gpower.com/businesses/ge\\_oilandgas/en/literature/en/downloads/sfs40.pdf](http://www.gpower.com/businesses/ge_oilandgas/en/literature/en/downloads/sfs40.pdf)
- [11] IEEE Std 115A, "IEEE Standard Procedures for Obtaining Synchronous Machine Parameters by Standstill Frequency Response Testing, 1987



**Stefan Schröder** (S'98 – M'03) was born in Cologne, Germany. He received the diploma and the doctoral degree both in electrical engineering from RWTH Aachen University, Aachen, Germany, in 1997 and 2003, respectively.

Since 1997, he has been a Research Associate at the Institute for Power Electronics and Electrical Drives (ISEA), RWTH Aachen University, where he was working on power electronic circuits and devices in particular on high-power semiconductors. Since July 2002, he has been Chief Engineer at the same

institute responsible for the research in the fields of electrical drives, power electronic circuits and semiconductor devices. Since the beginning of 2005, he is with GE Global Research Europe, Munich, Germany, where he is working on power electronic applications with focus on high-power converters for medium-voltage drives and for renewable energy systems.

He has authored or coauthored over 30 published technical papers. Dr. Schröder is a member of VDE.



**Pierluigi Tenca** (S'94–M'97) was born in Genova, Italy. He received the M.S. degree in electronic engineering and the Ph.D. degree in electrical engineering on power electronics topics (low-power/high-frequency dc/dc converters and high-power voltage-source multilevel converters) from the University of Genova, Italy, in 1996 and 2000, respectively.

He spent part of his Ph.D. course as Visiting Staff in the Department of Electronic and Electrical Engineering, University of Bath, U.K. In February

2000, he joined Siemens AG Transportation Systems, in Erlangen, Germany as an R&D Engineer, dealing with multilevel high-power converters and drives for traction applications. While on sabbatical leave from Siemens, he was a Staff Researcher with Prof. Thomas A. Lipo at the University of Wisconsin, Madison, USA from March 2003 to September 2005. There, his main research topics involved current-source topologies for large-power wind turbines (USA-NREL grant), as well as marine propulsion systems using superconducting motors and multilevel converters. From September 2005 to February 2008, he worked to the new development and testing of modular clusters of medium-voltage VSI drives for synchronous motors in excess of 30 MW with Ansaldo Sistemi Industriali, in collaboration with the General Electric Company (GE Global Research Center, USA/Germany and GE Oil & Gas). In April 2008 he has joined the ABB Corporate Research Center in Västerås, Sweden.

He has authored or co-authored more than twenty papers in IEEE, IET and EPE publications. He is a member of the IEEE Industry Applications, IEEE Power Electronics, IEEE Circuits and Systems and IEEE Industrial Electronics Societies, as well as of the EPE Association.



**Tobias Geyer** (M'08) received his Dipl.-Ing. and Ph.D. degrees in Electrical Engineering from ETH Zurich, Switzerland, in 2000 and 2005, respectively.

From 2006 to 2008, he was with GE's Global Research Center in Munich, Germany, where he was a project leader working on control and modulation schemes for large electrical drives. In late 2008 he joined the Power Electronics Group of the University of Auckland, New Zealand, as a Research Fellow. His research interests are at the intersection of modern control theory, optimization and power electronics, including model predictive control,

hybrid systems, electrical drives and dc-dc conversion.



**Paolo Soldi** was born in S. Margherita Lig. (GE), Italy. He received the Master Degree in Electrical Engineering from the University of Genova, Italy, in 1998.

From 1998 to 2005 he was with Bombardier Transportation (formerly Adtranz) in Milan, Italy and Turgi, Switzerland, where he worked on power electronics and control for traction drives. Since May 2005, he has been with General Electric Global Research Europe, Munich, Germany, where he is working on power electronic systems for high power

applications, in particular for the Oil&Gas and traction industries.

Mr. Soldi is a member of the Italian Association for Electrical Engineering, Automation, Information Technologies and Telecommunication (AEIT).



**Luis J. Garcés** received his Doctor Degree from the Technical University of Darmstadt, Germany.

He joined GE Global Research as a Power Electronics Engineer in 1998. Currently he is working on the control for Power Electronic systems, including among others: high power, medium voltage, high frequency drives for high-speed compressor drives for LNG applications, Power distribution systems for aircraft, controllers for very high performance gradient amplifiers for MRI. Prior to his joining GE, he held research positions with Rockwell Automations and Schneider-Telemecanique, where he was involved on

the development of general purpose drives and servos for machine tools. Dr. Garcés has authored several papers and tutorials, and been granted 40 US patents.



**Richard Zhang** (S'95–M'99) was born in Yunnan, China, in 1968. He received his B.S. and M.S. degrees in electrical engineering from Tsinghua University, Beijing, China, in 1989 and 1993, respectively. He received his Ph.D. degree from Virginia Polytechnic Institute and State University in 1998.

Currently Richard Zhang is an executive in GE company and joined GE Oil & Gas business as the Global Electrification Leader. Prior to that he was with GE Global Research Center for ten years, and

was the lab manager of Electronic Power Conversion Lab for the last seven years. He led power electronics research in GE, serving all GE industrial businesses such as Oil & Gas, Energy, Aviation, Healthcare, Transportation, and Enterprise Solution, as well as for government agencies such as DARPA, Office of Naval Research, Army Research Lab, Air Force Research Lab and Department of Energy. The advanced power electronics research programs that he leads range from systems, circuits, and controls to packaging and SiC switches for a wide range of applications, such as large drives for Oil & Gas, wind and solar power converters, aircraft and ship power conversion, medical power electronics.

Richard won a Best Paper Award for publication on IEEE Transactions on Power Electronics and one IAS prize paper award. He has published over 30 conference and journal papers, and hold 11 patents. He served as an Associate Editor for IEEE Transactions on Power Electronics, and currently serves as an IEEE PELS Adcom member and Chairman of Industry Advisory Board for CPES.



**Tommaso Toma** is acting as Electrical Systems Design Manager, with GE Oil& Gas, in Florence since 2008. He has responsibility for requisition engineering for power generation systems and electric drives as well as product development. He spent 3 years as Team leader of the Variable Speed Drive System and New product introduction team being focused on large VSIDS applications and product development for LNG and NG markets. Mr. Toma worked as Electrical Design Engineer on GT/ST generation plants, and spent two years in a quality assignment as 6Sigma Black Belt.

Mr. Toma graduated with honors (Electrical Engineering 1999) from Pisa University.

**Paolo Bordignon**

Picture and biography not available at time of publication